ANNALI DI GEOFISICA, VOL. XXXIX, N. 6, December 1996

The June 12, 1995 microearthquake sequence in the city of Rome

Alberto Basili, Luciana Cantore, Massimo Cocco, Alberto Frepoli, Lucia Margheriti, Concetta Nostro and Giulio Selvaggi
Istituto Nazionale di Geofisica, Roma, Italy

Abstract
The earthquake of June 12, 1995 has been located using local and regional data (41°48.8′N, 12°30.8′E at a depth of about 11.5 km) a few kilometers inside the city limit of Rome, in its southernmost part. This is the first event that occurred in Rome for which instrumental data are available. The local magnitude estimated from digital recordings is M_L 3.6 and it was largely felt reaching intensity VI MCS. We constrained the focal mechanism by analyzing the *S*-wave polarization and it agrees well with the distribution of *P*-wave polarities. The fault plane solution shows a dominant strike slip mechanism (strike 275°, dip 70°, rake −140°). Seismic moment, $M_0 = 2.3 \pm 0.6\ 10^{21}$ dyne·cm, was computed from *S*-wave displacement spectra of horizontal components of ground motion digital waveforms. The corresponding source radius ranges between 200 and 500 m, depending on the assumed stress drop (100 bars or 10 bars, respectively). The earthquake was preceded by a M_L 2.6 foreshock. The seismic sequence lasted a few days during which 38 aftershocks were recorded. The seismicity pattern shows the characteristics of a mainshock-aftershock sequence, rather than swarm behavior which seems to characterize the activity of the neighboring seismogenic areas of the Alban Hills. We used a master event algorithm to locate some of the aftershocks. Results show that the relocated aftershocks are clustered in a small volume in proximity of the mainshock hypocenter.

Key words *microseismicity – Rome – seismic hazard*

1. Introduction

The seismic activity in two distinct seismogenic areas is relevant to the assessment of seismic risk in the city of Rome. The first area, the Central Apennines, is affected by moderate to large magnitude earthquakes, while the second is the Alban Hills volcanic complex, characterized by seismic swarms. Due to the different distances of these seismogenic areas from Rome, we refer to the former as regional and to the latter as local seismicity. Small magnitude local earthquakes also occur inside the city of Rome (Rovelli *et al.*, 1994); these events had never been recorded instrumentally before the June 1995 earthquake which is investigated in this study.

Figure 1 shows the distribution of large historical earthquakes that occurred in the Central Apennines (such as the earthquakes of 1349, 1461, 1654, 1805 and 1915) and the local events occurring in the Quaternary volcanic area of the Alban Hills, located 25 km southeast of Rome. In particular, local seismicity occurs in the zone of more recent (0.3 My) volcanic activity, and is characterized by seismic swarms lasting for days to more than one year, rarely exceeding magnitude 4 (Amato *et al.*, 1994). The hypocenters of these earthquakes

Mailing address: Dr. Alberto Basili, Istituto Nazionale di Geofisica, Via di Vigna Murata 605, 00143 Roma, Italy; e-mail: Basili@ingrm.it

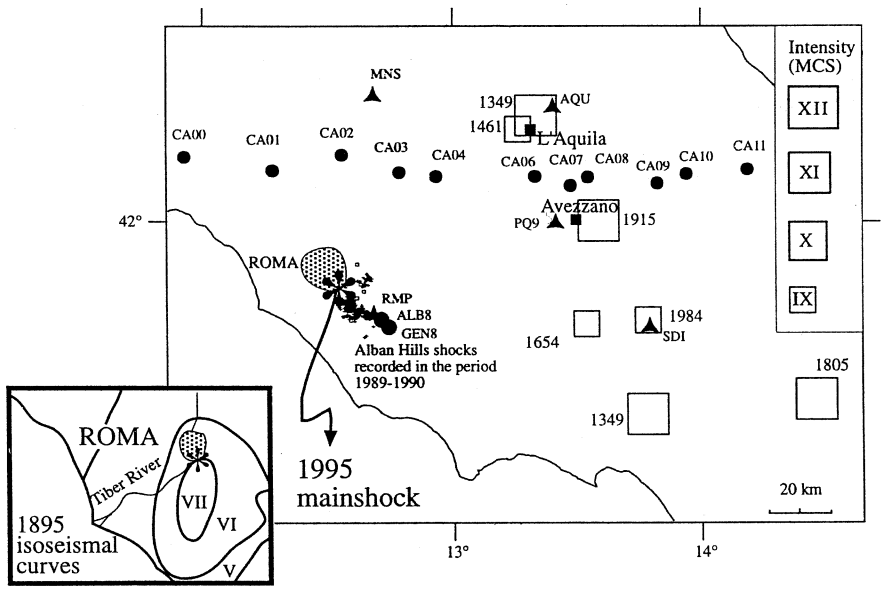

Fig. 1. Map of seismicity and location of the seismic stations that recorded the June 12, 1995 mainshock. Solid triangles indicate the vertical short-period seismometers of the ING National Network. Solid circles indicate the three component digital seismic stations (equipped either with short period, 5 s or broadband sensors). Open squares indicate the location of moderate-to-large historical earthquakes that occurred along the Apennines whose size scales with macroseismic intensity. The star shows the location of the 1995 mainshock. The distribution of epicenters of the 1989-1990 Alban Hills seismic swarms is also shown. The box in the bottom left corner shows the isoseismal curves of the 1895 earthquake (taken from Riguzzi and Tertulliani, 1993) that struck the same area as the 1995 event.

are concentrated in the first six kilometers of the upper crust (Amato *et al.*, 1994). Despite their small magnitudes, they are largely felt in Rome. The maximum macroseismic intensity felt in Rome due to either regional or local earthquakes is the VIII degree MCS (Molin and Guidoboni, 1989). In this paper we analyze the seismicity and the seismograms recorded during the June 12, 1995 (M_L 3.6) earthquake which occurred within the city of Rome (see fig. 1).

There exist several reports of historical events that occurred inside the city of Rome, such as March 22, 1812, November 1, 1895 and August 31, 1909, that also produced a maximum macroseismic intensity of VIII degree MCS (Molin *et al.*, 1986; Riguzzi and Tertulliani, 1993). The earthquakes of 1812 (Basili *et al.*, 1990) and 1895 (De Rossi 1897; Agamennone, 1924) were located in the southwestern part of the town while the event of 1909 was located in the northeastern part (Martinelli, 1909). We have plotted in fig. 1 (see the box at the bottom left corner) the isoseismal curves of the 1895 seismic event (taken by Riguzzi and Tertulliani, 1993) together with the 1995 epicenter. The 1895 earthquake is particularly important because it struck the same area where the 1995 event was largely felt.

Although earthquakes in Rome are less frequent than in the Alban Hills, they are equally important to determine the distribution of seismicity in the area and to assess the seismic hazard in the city of Rome. Moreover, we provide a comparison between the temporal and spatial seismicity patterns of the 1995 and the Alban Hills seismic sequences. We note that this earthquake is the largest event ever recorded which occurred inside the city of Rome.

2. Mainshock location and magnitude

The mainshock occurred on June 12, 1995 at 18:13 (GMT) and was mainly felt in the southern part of Rome causing little damage (I_0 = VI MCS) and panic in the population. The local magnitude (M_L 3.6) has been computed from the ground motion recordings of digital three-components seismic stations. It was recorded by the stations of the permanent seismic network (Teledyne S-13 vertical seismometers) of the Istituto Nazionale di Geofisica (ING), by three digital short period three-component stations installed in the Alban Hills, and by 11 digital three-component seismic stations (Guralp CMG4 and LE/3D C 5s) deployed by ING during a teleseismic transect experiment (Amato *et al.*, 1995).

Figure 1 shows the distribution of seismic stations that recorded the mainshock, and fig. 2

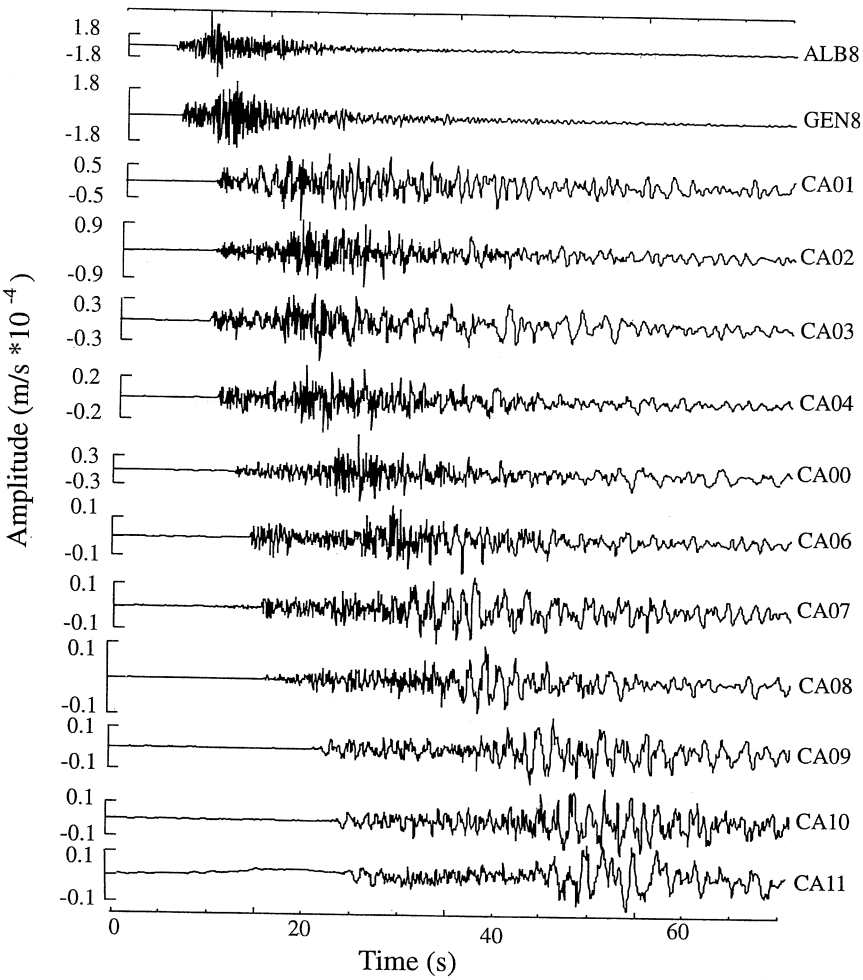

Fig. 2. Vertical components of ground velocity recorded at several seismic stations during the June 12, 1995 mainshock.

Table I. Velocity model used to locate the mainshock.

V_p (km/s)	Top of the layer depth (km)
5.8	0.0
6.8	12.0
8.1	30.0

shows the vertical components of the seismograms recorded by several stations located at increasing epicentral distances. The number of available recording stations allows the mainshock hypocenter to be located: it occurred at 41°48.8′N and 12°30.8′E at a depth of 11.5 km, in the southern part of the city. We use the velocity model shown in table I, and the code Hypoinverse (Klein, 1989) to locate the earthquake. The formal errors are within 1 km and the root mean square of the residual is equal to 0.23 s. We locate this seismic event using different velocity models; these tests show that the hypocentral locations are comparable and, in particular, that the hypocenter is deeper than 10 km (the preferred locations is at 11.5 km depth). Worthy of note is the observation that the 1995 mainshock is remarkably deeper than the Alban Hills seismic events (located at depths ranging between 3 and 6 km).

We have computed the seismic moment from the *S*-wave displacement spectra of horizontal components of ground motion recorded at the digital broadband seismic stations. The resulting average value is $M_0 = 2.3 \pm 0.6\ 10^{21}$ dyne·cm, that corresponds to a moment magnitude (Hanks and Kanamori, 1982) of $M_W = 3.5$. This moment magnitude value is very similar to the estimated local magnitude (M_L). It is difficult to estimate the stress drop of this event from the recorded data, because at this small magnitude the effect of anelastic attenuation complicates measurement of the corner frequency either from ground acceleration spectra or, in time domain, from the displacement pulse. However, an attempt to estimate the corner frequency from *S*-wave spectra, provides an f_c value close to 2.5 Hz, that yields a Brune stress drop of roughly 10 bars. The source radius r can be computed by means of the following equation

$$r^3 = \frac{7}{16}\frac{M_0}{\Delta\sigma}$$

where $\Delta\sigma$ is the stress drop. For a stress drop ($\Delta\sigma$) ranging between 10 and 100 bars, the resulting source radius ranges between 200 and 500 m. The expected corner frequencies associated to these values of the source radius can be estimated by using the following relation

$$f_c = 2.34\frac{\beta}{2\pi r}$$

where β is the *S*-wave velocity; their values range between 2.3 and 6 Hz. We speculate a roughly 500 m fault radius and a corner frequency of 2.5 Hz can be considered reliable estimated source parameters for the 1995 earthquake.

3. Mainshock fault plane solution

We determined the fault plane solution of the mainshock from the first motion *P*-wave polarities observed at those stations having a clear onset of the *P*-waves arrival, using the FPFIT code (Reasenberg and Oppenheimer, 1985). Because of the large azimuthal gap (~ 180°), we obtained two equally probable solutions, that are shown in fig. 3. Note that both the solutions have a *T* axis oriented NE-SW, in agreement with the general extension observed both in the Apennines and in the Volcanic region, and resulting from focal mechanisms and borehole breakout data (Gasparini *et al.*, 1985; Deschamps and King, 1984; Anderson and Jackson, 1987; Ward and Valensise, 1989; Amato *et al.*, 1994; Montone *et al.*, 1995).

The availability of three-component digital seismic stations offered us the opportunity to constrain the focal mechanism by analyzing the *S*-wave polarization (Zollo and Bernard, 1991). This approach requires that the observed *S*-wave polarization directions reflect the source mechanism. In fact, the polarization can be affected by site effects, anisotropy, head

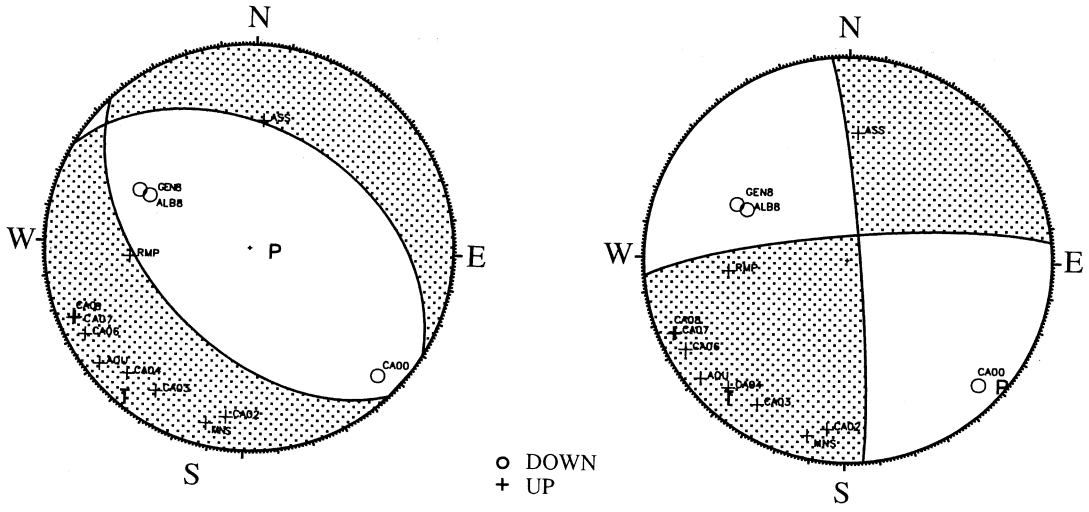

Fig. 3. Two equally probable fault plane solutions obtained by inverting the observed *P*-wave polarities (strike 135°, dip 50°, rake – 80°; strike 265°, dip 80°, rake 170°).

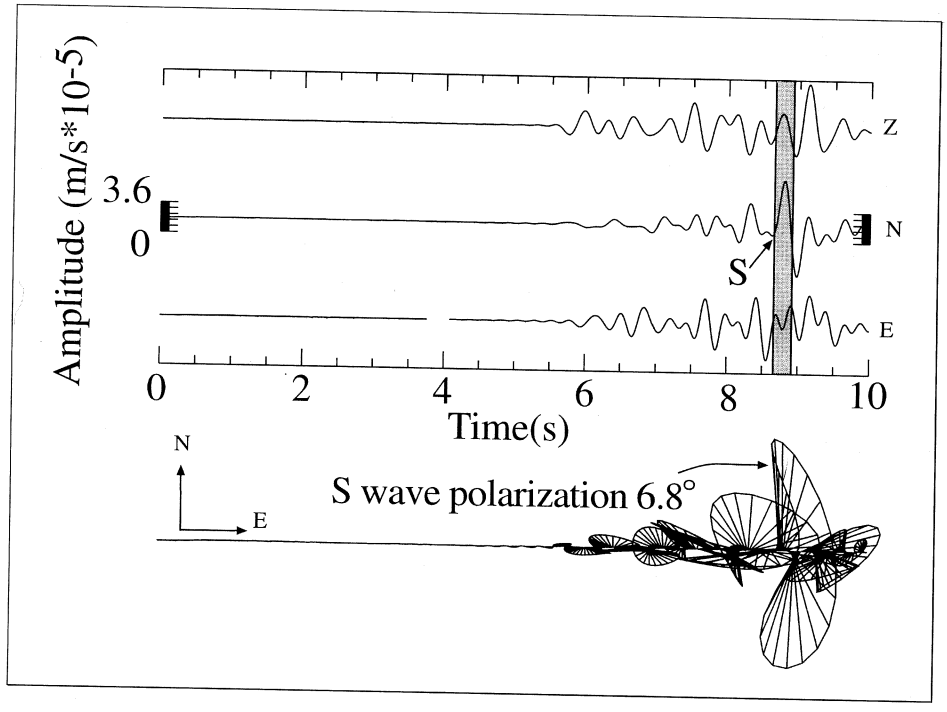

Fig. 4. Example of computation of *S*-wave polarization at the GEN station using the covariance matrix decomposition method. Ground velocity was pass-band filtered between 0.2 and 4.0 Hz.

waves and converted phases. For each seismic station, we compared the direction of the *P*-wave polarization with the back-azimuth resulting from the mainshock location to verify the absence of significant site effects, that could introduce a directional amplification of the ground motion that might affect the observed polarization direction (Bonamassa and Vidale, 1991). Thus, we used only those stations for which these two directions are similar. We also verified that, for the selected stations, we are within the *S*-wave window, and that the polarization of the first *S*-wave arrival was not affected by seismic anisotropy checking that it changes at the same station for different earthquakes. Finally, we selected six stations for the polarization analysis. To determine the *S*-wave polarization we adopted the covariance matrix decomposition method (Jurkevics, 1988; Zhang and Schwartz, 1994; Margheriti *et al.*, 1996). Figure 4 shows an example of application of the covariance matrix decomposition method to estimate the *S*-wave polarization at the station GEN; the observed polarization was computed using all three components of the ground motion time history.

By using a grid search procedure we selected those fault plane solutions for which the difference between the theoretical and the observed *S*-wave polarization was less than 25°. At each iteration we changed the strike dip and rake by 5° and we computed the theoretical *S*-wave polarization for each seismic station. Only one fault plane solution reproduced the *S*-wave polarization observed at all six selected stations. The theoretical and observed values are listed in table II. The focal mechanism resulting from the polarization analysis is shown in fig. 5. This fault plane solution (strike 275°, dip 70°, rake – 140°) is very similar to one of the two obtained by inverting the first motion polarities (fig. 3). Worthy of note is the good agreement between the nodal planes constrained by the analysis of *S*-wave polarization and the distribution of the *P*-wave polarities.

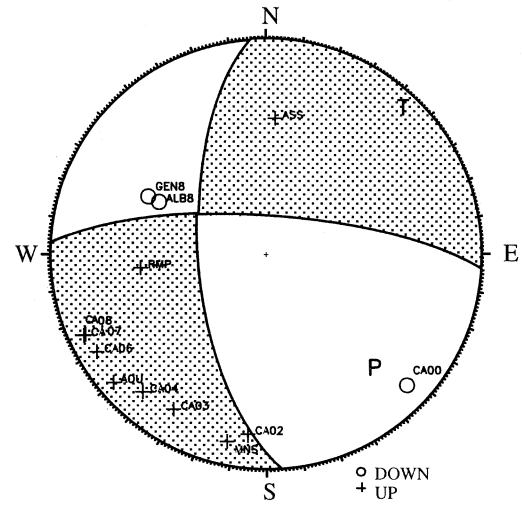

Fig. 5. Fault plane solution resulting from the analysis of *S*-wave polarization (strike 275°, dip 70°, rake – 140°). First motion *P*-wave polarities have been plotted for comparison.

Table II. Theoretical and observed *S*-wave polarization.

Station	Theoretical *S*-wave polarization (°) (strike 275°, dip 70°, rake – 140°)	Observed *S*-wave polarization (°)
GEN	24.5	6.8
ALB	23.4	22.1
CA03	125.2	150.1
CA04	296.3	316.0
CA06	329.7	314.0
CA08	328.7	307.0

4. Temporal and spatial distribution of the aftershocks

The June 12, 1995 mainshock was preceded by a M_L 2.6 foreshock which occurred about one hour before (17:07 GMT), and was followed by several aftershocks. The seismic sequence lasted for a few days during which we recorded 38 aftershocks with magnitudes ranging between 1.6 and 2.9. Figure 6 shows the temporal distribution of seismicity and the magnitudes of the largest aftershocks. Such a distribution is characteristic of mainshock-aftershock sequences rather than seismic swarms, that are generally observed in the seismogenic areas of the Alban Hills. Figure 7 shows the spatial distribution of seismicity of the 1995 seismic sequence and of the 1989-1990 Alban Hills seismic swarms. Most of the 1995 aftershocks occurred inside the city limit of Rome (that corresponds to the GRA freeway shown in fig. 7). The aftershock epicenters show a large

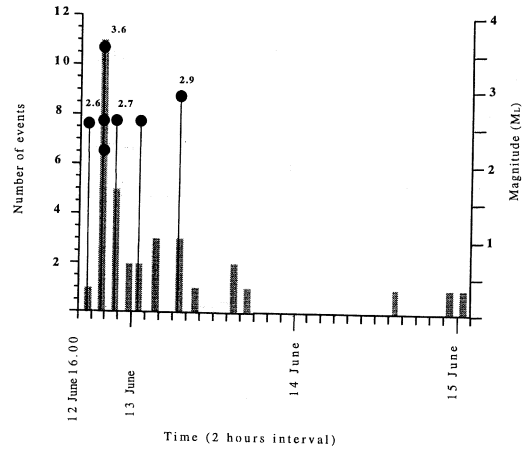

Fig. 6. Temporal distribution of seismicity during the 1995 sequence. The right axis shows the local magnitudes computed for the largest aftershocks (solid circles), while the left axis shows the number of events (gray columns). Time interval on the abscissa is two hours.

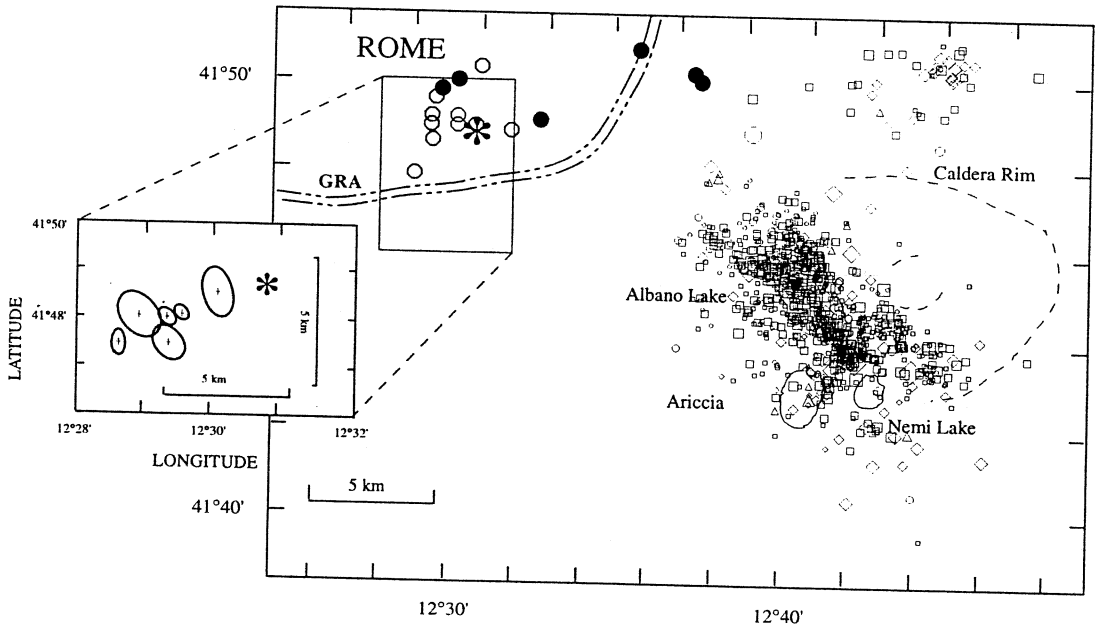

Fig. 7. Spatial distribution of seismicity of the 1995 sequence and of the 1989-1990 Alban Hills seismic swarm. The solid circles indicate those events that were selected for relocation using the master-event method. The box on the left shows the epicenters of these relocated aftershocks, ellipses indicate the formal errors.

dispersion due to the small number of readings available for these small magnitude events.

For this reason, we used a master event algorithm to investigate their spatial distribution (Westaway, 1992). We considered the mainshock the master event. This method is based on the assumption that the ray path from the source to the recording station is the nearly the same for the selected master event and for the aftershocks. This assumption was verified for stations sufficiently far away from the hypocenter, and in case of closely located master and secondary events. In this case the difference in arrival times at each station is only due to the origin time and to the master to secondary hypocentres distances. The same hypocentral depth for the mainshock (master event) and the aftershocks was assumed. We relocated only those secondary earthquakes for which at least five arrival times in common with the mainshock were available. The solid circles in fig. 7 indicate the six events selected for the relocation. This subset of data includes the 2.6 magnitude foreshock and the largest five aftershocks.

After relocation the selected aftershocks appear clustered in a small volume (fig. 7, box in the left bottom corner); the ellipses indicate the errors of relocation. By analyzing the difference in arrival times between P and S waves at those stations that recorded either the mainshock and the aftershocks, we conclude that most of the aftershocks are clustered as expected for a microearthquake seismic sequence and located east of the mainshock; noting that the ellipses are smaller than the relative distances between the relocated events, we consider their distribution representative of an activated area elongated about EW.

5. Discussion and conclusive remarks

An analysis of historical earthquakes and of the June 12, 1995 seismic sequence clearly demonstrates that earthquakes occur inside the city of Rome. The 1995 earthquake struck the same area where the 1895 event occurred. This area has been intensely populated in the last decades (roughly 600000 people live there), thus the social impact of the 1995 earthquake was much more than that expected for a magnitude 3.6 earthquake. The recordings of digital ground motion waveforms of the June 12, 1995 seismic sequence provided a unique opportunity to study these earthquakes in detail.

Because of the vicinity of the Alban Hills, the earthquakes of Rome and the 1995 seismic sequence could belong to the same seismogenic area or show the same seismicity pattern. Results of this study demonstrate that this is not true. In particular, the earthquakes of the 1995 sequence were deeper than those of the 1989-1990 Alban Hills seismic swarm. The mainshock was located at 11.5 km of depth; thus it is deeper than the Alban Hills seismic events that were located in the first six kilometers of the upper crust. Moreover, the 1995 earthquakes were located north of the seismogenic area where the 1989-1990 Alban Hills swarms occurred. The temporal pattern of the sequence is clearly different from the seismic swarm behavior characteristic of the Alban Hills sequences. The 1995 sequence showed a temporal pattern more similar to a mainshock-aftershock sequence then to a seismic swarm.

We estimated the local magnitude and the seismic moment of the June 12, 1995 mainshock from the recorded digital waveforms: their values were M_L=3.6 and M_0=2.3 $\pm$ 0.6 10^{21} dyne·cm, respectively. The corresponding moment magnitude was M_W = 3.5. The resulting source radius ranged between 200 and 500 m depending on the adopted stress drop values (100 bars or 10 bars respectively).

The fault plane solution shows an oblique mechanism with a dominant right lateral strike slip component (strike 275°, dip 70°, rake – 140°) on the EW plane; relocated aftershocks are clustered in a small volume elongated about EW. This focal mechanism is consistent with the direction of extension observed both in the Apennines and in the peri-tyrrhenian volcanic region as resulting from focal mechanisms and borehole breakout data (Montone *et al.*, 1995). Despite the small magnitude and source radius of the June 12, 1995 earthquake, its fault plane solution is also consistent with the presence of EW and NS planes suggested by Marra and Rosa (1995) to explain the recent evolution of Pleistocenic basins in the roman area.

This is the first time that recordings of an earthquake M_L = 3.6 located in Rome have been available; this gives us the possibility to study the sequence and to define some major characteristics of the seismicity in the city to better assess the potential seismic hazard inside the urban area.

Acknowledgements

We thank Fabrizio Marra and Paola Montone and the ING macroseismic group for helpful discussions. Special thanks to Alessandro Amato and to the ING research group that deployed the teleseismic Transect for providing the data used in this study. We thank Claudio Chiarabba, Aldo Zollo and an anonymous referee for reviewing the manuscript. Luciana Cantore was supported by a CNR fellowship when she worked at ING. Concetta Nostro and Lucia Margheriti were supported by the European Community (EV5V-CT94-0464).

REFERENCES

AGAMENNONE, G. (1924): Contributo allo studio del terremoto romano del 1 novembre 1895, *Boll. Soc. Sism. Ital.*, **24**, 89-91.

AMATO, A., C. CHIARABBA, M. COCCO, M. DI BONA and G. SELVAGGI (1994): The 1989-1990 seismic swarm in the Alban Hills volcanic area, Central Italy, *J. Vol. Geotherm. Res.*, **61**, 225-237.

AMATO, A., R. AZZARA, M.G. CIACCIO, G.B. CIMINI, C. CHIARABBA, M. DI BONA, A. FREPOLI, L. MARGHERITI, C. NOSTRO and G. SELVAGGI (1995): Deep structure beneath the Northern Apennines (Italy) from passive seismological studies, IUGG 2-14 July 1995 Boulder, Colorado, volume abstract SA41D-08.

ANDERSON, H. and J. JACKSON (1987): Active tectonics of the Adriatic region, *Geophys J. R. Astron. Soc.*, **91**, 937-987.

BASILI, A., P. FAVALI, G. SCALERA and G. SMRIGLIO (1990): An attempt to evaluate seismic hazard in Central-Southern Italy, *Natural Hazard*, **3**, 31-47.

BONAMASSA, O. and J.E. VIDALE (1991): Directional site resonance observed from aftershocks of the 18 October 1989 Loma Prieta earthquake, *Bull. Seism. Soc. Am.*, **81** (5), 1945-1957.

DE ROSSI, M.S. (1897): I terremoti nella città di Roma, *Bull. Vulc. Ital.*, **18-20**, 9-21.

DESCHAMPS, A. and G.C.P. KING (1984): Aftershocks of the Campania-Lucania earthquake of 23 November 1980, *Bull. Seism. Soc. Am.*, **74**, 2483-2517.

GASPARINI, C., G. IANNACCONE and R. SCARPA (1985): Fault-plane solutions and seismicity of the Italian peninsula, *Tectonophysics*, **117**, 59-78.

HANKS, T.C. and H. KANAMORI (1979): A moment magnitude scale, *J. Geophys. Res.*, **84**, 2348-2350.

JURKEVICS, A. (1988): Polarization analysis of three-component array data, *Bull. Seism. Soc. Am.*, **78**, 1725-1743.

KLEIN, F.W. (1989): Hypoinverse, a program for vax computers to solve for earthquake location and magnitude, *USGS Open-file Report*, 89-314, 6/89 version.

MARGHERITI, L., C. NOSTRO, M. COCCO and A. AMATO (1996): Seismic anisotropy beneath the Northern Apennines (Italy) and its tectonic implications, *Geophys. Res. Lett.*, **23** (20), 2721-2724.

MARRA, F. and C. ROSA (1995): Stratigrafia e assetto geologico dell'area romana, in *La Geologia di Roma. Il Centro Storico*, Mem. Descr. della Carta Geol. D'It., **50**, Ist. Poligrafico e Zecca dello Stato.

MARTINELLI, G. (1909): Notizie sui terremoti osservati in Italia durante l'anno 1909, *Boll. Soc. Sism. Ital.*, **16**, 447-459.

MOLIN, D. and E. GUIDOBONI (1989): Effetto fonti e effetto monumenti a Roma: i terremoti dall'antichità a oggi, in *I Terremoti Prima del Mille in Italia e nell'Area Mediterranea*, edited by E. GUIDOBONI (SGA, Bologna), 194-223.

MOLIN, D., S. AMBROSINI, S. CASTENETTO, E. DI LORETO, L. LIPARI and A. PACIELLO (1986): Aspetti della sismicità storica di Roma, *Mem. Soc. Geol. It.*, **35**, 439-448.

MONTONE, P., A. AMATO, C. CHIARABBA, G. BUONASORTE and A. FIORDELISI (1995): Evidence of active extension in Quaternary volcanoes of Central Italy from breakout analysis and seismicity, *Geophys. Res. Lett.*, **22**, 1909-1912.

REASENBERG, P.A. and D. OPPENHEIMER (1985): Fortran computer programs for calculating and displaying earthquake fault-plane solutions, *USGS Open-file Report*, 85-739, 109.

RIGUZZI, F. and A. TERTULLIANI (1993): Re-evaluation of minor events: the examples of the 1895 and 1909 Rome earthquakes, *Natural hazard*, **7**, 219-235.

ROVELLI, A., A. CASERTA, L. MALAGNINI and F. MARRA (1994): Assessment of potential strong ground motions in the city of Rome, *Annali di Geofisica*, **37**, 6-12.

WARD, S.N. and G.R. VALENSISE (1989): Fault parameters and slip distribution of the 1915 Avezzano, Italy, earthquake derived from geodetic observations, *Bull. Seism. Soc. Am.*, **79**, 690-710.

WESTWAY, R. (1992) Seismic moment summation for historical earthquakes in Italy: tectonic implications, *J. Geophys. Res.*, **97** (B11), 15437-15464.

ZHANG, Z. and Y. SCHWARTZ (1994): Seismic anisotropy in the shallow crust of the Loma Pietra segment of the San Andreas fault system, *J. Geophys. Res.*, **99**, 9651-9661.

ZOLLO, A. and P. BERNARD (1991): Fault mechanisms from near source data: joint inversion of *P* polarities and *S* polarization, *Geophys. J. Int.*, **104**, 441-451.

(received March 14, 1996;
accepted September 2, 1996)